

Sustainability evaluations on material consumption for terawatt-scale manufacturing of silicon-based tandem solar cells

Li Wang¹ | Yuchao Zhang¹ | Moonyong Kim¹  | Matthew Wright² | Robert Underwood¹ | Ruy Sebastian Bonilla² | Brett Hallam¹ 

¹UNSW Sydney, Sydney, NSW, Australia

²Department of Materials, University of Oxford, Oxford, UK

Correspondence

Li Wang, UNSW Sydney, Sydney, NSW 2052, Australia.

Email: li.wang3@unsw.edu.au

Funding information

Australian Centre for Advanced Photovoltaics; Australian Renewable Energy Agency, Grant/Award Number: 2020/RND005; Royal Academy of Engineering; UK Engineering and Physical Sciences Research Council, Grant/Award Number: EP/V038605/1; John Fell Fund at Oxford University

Abstract

High-efficiency silicon-based tandem solar cells will likely drive the push towards terawatt (TW) scale PV manufacturing on the pathway to net zero emissions by 2050. In this work, we provide a comprehensive analysis of material consumption and sustainability issues for future tandem solar cells. First, we analyse the material consumption and sustainable manufacturing capacity of a variety of potential candidates for the top cell in a silicon-based tandem cell. We show that III-V, CIGS and CdTe are not suitable to support TW-scale manufacturing. Perovskites thus present the most sustainable approach, as long as indium is not required in the cell structure. Next, we turn our attention to the silicon bottom cell architecture by comparing PERC, TOPCon and SHJ. Although tandem cells can generally reduce silver consumption relative to single junction silicon cells due to the more favourable J_{MP}/V_{MP} ratio, the PERC cell architecture could allow for significantly reduced Ag consumption compared with both TOPCon and SHJ by relying on Al for the rear p-type contact. In order to drive a rapid shift towards TW-scale manufacturing, a rapid upscaling compared with the current production capacity is needed. The results presented herein highlight the need for careful consideration of sustainability issues when designing future high-efficiency tandem cells that will help the world mitigate the dangers of climate change.

1 | INTRODUCTION

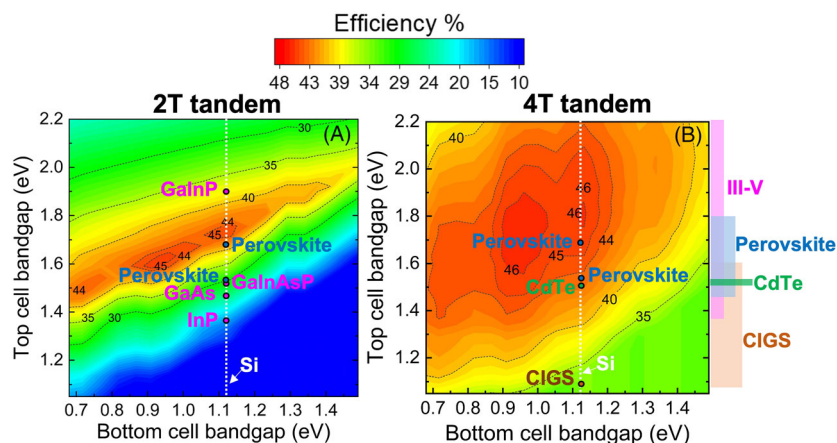
In order to mitigate the impact of climate change, the average global temperature increase relative to preindustrial times must be limited to well below 2°C or preferably less than 1.5°C.¹ Failure to do so could lead to increased intensity and frequency of extreme weather events, loss of biodiversity and significant impacts to the livelihood of billions of people.² The most effective way to reduce CO₂ emissions is to

replace fossil fuels for electricity production with renewable energy. Over the last 15 years, the cost of electricity from solar photovoltaics (PV) has plummeted,³ making solar PV the most viable technology to replace fossil fuels. The annual production of solar PV modules in 2021 was 191 GW; however, this must be rapidly increased to achieve the required reduction in CO₂ emissions. It has been predicted that production needs to be increased to 1 TW p.a. by 2030 and ideally as high as 3 TW p.a. to avoid a major downturn of

This is an open access article under the terms of the [Creative Commons Attribution-NonCommercial-NoDerivs](https://creativecommons.org/licenses/by-nc-nd/4.0/) License, which permits use and distribution in any medium, provided the original work is properly cited, the use is non-commercial and no modifications or adaptations are made.

© 2023 The Authors. Progress in Photovoltaics: Research and Applications published by John Wiley & Sons Ltd.

FIGURE 1 Shockley–Queisser detailed balance efficiency as a function of subcell band gaps for (A) 2T and (B) 4T configurations. White dot lines represent the bandgap of Si bottom cell; colour dots represent the bandgaps of selected cell candidates studied in this work. Bandgap ranges for each cell type are labelled by coloured bars along the y-axis of (B).



replacing end-of-life modules on the pathway to net zero emissions by 2050.^{4–7} This rapid expansion of production volume introduces a new challenge in designing solar cells. Over the past 20 years, the solar industry has significantly improved solar panels with the primary goal of increasing the efficiency and reducing production costs. However, the requirement for at least 1 TW of annual production in the near future means that the material consumption must also be urgently considered. To expand the solar PV industry in a sustainable manner, thought must be given to the material consumption for the materials that go into forming the solar cell, as well PV modules and balance of systems components. Additionally, the environmental and social impacts during the entire process of material production should be considered. Therefore, it is of great importance and urgency to understand the availability and present consumption of materials required by PV, to evaluate the feasibility of TW-scale expansion and prevent material availability crises in the future.

The single junction silicon PV market is currently dominated by the passivated emitter and rear cell (PERC) design; however, the increased efficiency potential of tunnel oxide passivated contact (TOPCon) and silicon heterojunction (SHJ) cell architectures has raised significant commercial interest. Despite their promise, the practical efficiency limit for a single junction silicon solar cell is 29.4%, based on the band gap (E_g) and limitations of Auger recombination.⁸ The world record efficiency of 26.81%, which was achieved with a SHJ architecture, is approaching the practical limit for a single junction silicon cell.⁹ A key approach to reduce the levelized cost of electricity (LCOE) from solar PV, which will help to further accelerate deployment, is to increase the efficiency. This is particularly true when the balance of systems (BOS) cost of installations is area dependent, such as in the residential PV market.¹⁰ Tandem solar cells, where two solar cells with different band gaps are combined together, represent the best way to increase the efficiency, overcoming the ~30% efficiency limit barrier of single junction solar cells. A tandem solar cell with two subcells has a theoretical efficiency limit of ~46% based on Shockley–Queisser detailed balance limit, which represents a significant potential efficiency gain over single junction devices.¹¹ An additional benefit of the tandem cell approach is the potential to reduce the material consumption, which can be quantified in terms of ‘mg/W’. To improve this mass-to-power ratio, it is ideal to reduce the mass of

materials consumed and increase the power output of the module, by increasing the efficiency.

The market for silicon solar cells is well established and is built on more than 20 years of manufacturing learning experience. In the short term to midterm, the most viable bottom cell design for commercial production will therefore be silicon based. With a band gap energy (E_g) of 1.12 eV at 300 K, silicon is well suited as a bottom cell from both a technical perspective and a manufacturing perspective, the upper limit on efficiency for a silicon-based tandem cell is ~43%.¹² This means it is critically important to identify the most appropriate top cell material to couple with silicon. The most important material property to optimise the efficiency of a tandem solar cell is the E_g . Figure 1 displays the Shockley–Queisser detailed balance efficiency limit for a tandem cell with either a two-terminal (2T) or four-terminal (4T) design, as a function of the top cell E_g . Figure 1A describes the 2T case, where the two cells are monolithically integrated and connected in series. For this case, where the cells are electrically coupled, current matching is required between the two cells to maximise the efficiency. When we assume the bottom cell is silicon, with E_g of 1.12 eV, the achievable efficiency ranges from 35% to 45% when the top cell E_g varies from 1.6 to 1.95 eV. Figure 1B displays the detailed balance efficiency for tandems with a 4T arrangement, such that the two cells are mechanically stacked together. In the 4T case, the cells are optically coupled, as they share the same illumination source; however, they are not electrically coupled so that current matching is not required. This significantly broadens the range of top cell E_g that can achieve high efficiency. The most promising material choices for the top cell include III-V, CIGS, CdTe and perovskites. The range of available E_g for each material and E_g for selected candidates of this work is displayed in Figure 1. III-V solar cells have consistently achieved high efficiencies, from 24.2% InP cell¹³ to 29.1% efficient GaAs cell,¹⁴ then 35.9% efficient GaInP/GaInAsP/Si¹⁵ triple junction solar cell, which is the highest reported efficiency to date for Si-based multijunction solar cell technologies. As an established technology, CdTe cells have achieved 22.1% efficiency.¹⁶ Due to the toxicity of Cd, Cd-free CIGSe cells have been developed and achieved a higher efficiency of 23.35%.¹⁷ Most recently, the rapid development of perovskite cells has demonstrated world record efficiencies of 25.8%,¹⁸ 32.5%¹⁹ and

30.1%²⁰ for single junction perovskite, 2T perovskite/Si tandem and 4T perovskite/Si tandem devices, respectively.

The vast majority of prior research on tandem cell designs has focussed on improving the efficiency. However, as the market rapidly transitions to TW scale, sustainability considerations must now be brought to the forefront. Regarding the top cell design, most of the likely candidates include scarce materials, such as gallium, indium, tellurium and selenium, while some require toxic materials, such as lead or cadmium. Depending on the cell architecture and interconnection scheme, indium is required in the form of indium tin oxide (ITO) as a transparent conducting oxide (TCO) layer. The most common metallisation approach for high-efficiency single junction cells and perovskite/Si tandems is screen printing of silver, which can also cause scarcity issues. Some recent reports have raised the alarm regarding material consumption for PV manufacturing. Till et al. discussed the shortage of indium for thin-film technologies.²¹ Raw material needs for PERC, SHJ, CIGS and III-V/Si modules were investigated thoroughly, and supply risks based on a material demand-to-production comparison have been identified.²² Kamaraki et al.²³ calculated the time it would take to produce the required materials to create 1–30

TW of PV from selected state-of-the-art cell architectures at the current rate of global primary production. Sustainable manufacturing capacity (SMC) of commercial silicon cell technologies imposed by silver, indium and bismuth was evaluated by Zhang et al.²⁴

In this report, we provide the first thorough analysis of the sustainability issues regarding material consumption for silicon-based tandem solar cells. We do this by calculating material consumption in mg/W for each possible component. Based on the availability of each material, the sustainable manufacturing capacity for each technology is then calculated with the aim of TW-scale manufacturing in mind. The analysis investigates the critical material usage for various top cell candidates (III-V, CIGS, CdTe and Perovskite), Si bottom cells candidates (PERC, TOPCon and SHJ) and associated silver metal requirement and lateral transport/buffer layers typically based on ITO for SHJ, perovskite and perovskite/Si tandem solar cells. From this, SMC of various Si-based tandem architectures is estimated, gaps between target and actual material consumptions are identified and opportunities to reduce the consumptions are explored, to provide valuable evaluation on feasibility of TW-scale manufacturing and consideration for future sustainable tandem designs.

TABLE 1 Cell type, efficiency and material thickness used for estimating the consumption of critical elements.

Cell type	Material	Efficiency (%)	Thickness (nm)	Ref
III-V and III-V/Si	GaAs	29.1	1000	14
	InP	24.2	5200 (InP)	13
	GaInP/GaInAsP/Si	35.9	530 (Ga _{0.51} In _{0.49} P)	15
			1680 (Ga _{0.93} In _{0.07} As _{0.87} P _{0.13}) 700 (Al _{0.06} Ga _{0.94} As)	
CIGS	CuIn _{0.9} Ga _{0.1} Se ₂	23.35	1000–2500	17
CdTe	CdTe	22.1	2000–8000 (CdTe)	16,25
			60–200 (CdS)	
Perovskite and perovskite/Si	FAPbI ₃	25.8	300–700. FAPbI ₃ and Cs _{0.05} (FA _{0.77} MA _{0.23}) _{0.95} Pb(I _{0.77} Br _{0.23}) ₃	18 (Tables S2 and S3)
	In in ITO layer		40–285 (ITO) on perovskite only	
PERC	Silicon and Ag	22.99–24.5	Si: wafer thickness 150–167 µm, cell sizes 16.6 × 16.6 = 275.56 cm ² and 21 × 21 = 441 cm ² ; Ag:	9,24,26–28
TOPCON	Silicon and Ag	23.71–26.1	cell metallisation patterns as our previous work, nine busbars for 275.56 cm ² and 12 busbars for 441 cm ²	
SHJ	Silicon and Ag	24.02–26.81	In: 70- to 100-nm ITO for each side of SHJ cells, 275.56 and 441 cm ²	
Perovskite/Si	Silicon	32.5	Si bottom cell 170–300 µm. Assumed the highest efficiency of 32.5%	19 (Tables S2 and S4)
	Ag		Ag: assume the same pattern as for the single junction PERC, TOPCon and SHJ but with a tandem efficiency of 32.5%	
Perovskite/Si	In in ITO layer	2T: 24.5–32.5% 4T: 25.2–30.1%	Interconnection and lateral conductors on perovskite/Si tandem 2T: 40–320 nm 4T: 145–480 nm	Tables S2 and S3

2 | METHODOLOGY

Various cell types with world-record efficiencies above 22% were selected as the top cell candidates and are listed in Table 1. In order to obtain a range of critical element consumption in mg/W primarily from the thicknesses of absorbing layers and buffer layers in the cell architectures, the following cell technologies were selected: three representative cell architectures from the III-V group, the highest efficiencies and a range of thicknesses for CIGS and CdTe candidates, a perovskite single junction with champion efficiency and a wide range of perovskite/Si tandem candidates. Literature values were used for the absorbing layers thicknesses of perovskites, ITO thicknesses both on perovskite cell and on the whole tandem device and silicon bottom cell thicknesses. In addition, the thicknesses of 150 and 167 μm and wafer sizes of M6 and M12 were used for single junction silicon solar cells from Infolink²⁶ and 2021 results of International Technology Roadmap for Photovoltaic (ITRPV) 2022.²⁹ The average efficiencies in mass production reported in ITRPV 2022 and large-area champion or world-record efficiencies for PERC,²⁷ TOPCon²⁸ and SHJ⁹ cells were used. Two silver metallisation patterns, consisting of 9 busbars and 12 busbars for M6 size and M12 size, respectively, were referenced from our previous work²⁴ with updated finger widths as shown in Table S4. A material utilisation rate of 80% was assumed for the material growth for III-V, CIGS, CdTe and perovskite candidates and sputter target material efficiency for ITO deposition. It is worth noting that 80% is only considering material utilisation rate from the sputter targets,²⁹ there are further material losses associated with material loss on wafer carriers or in the chamber, which results in overall sputter material utilisation efficiency below 60% according to a physical vapour deposition (PVD) equipment supplier. A utilisation rate of 68% was assumed for Si considering kerf losses during wafering process and other material losses during cell fabrication process.³⁰

Material consumption (C_x , in mg/W) was calculated using Equation (S1). Here, we assumed total available material supply (S_x , in tonnes/year) was equivalent to only 20% of 2020 global primary material supply based on US Geological Survey³¹ for each critical material listed in Table 1. It is unclear precisely what percentage of global material annual supply is a “sustainable” number for PV to consume. It is also difficult to assess how much of the materials should be consumed by PV. However, as the cost of PV is so low and the lifespan is so long (25–30 years), it is not reasonable for PV to take considerable amount of scarce and precious materials during the whole lifespan. In addition, if the material demands are much higher than the supplies, even small price fluctuations will have dramatic impact on PV due to its relatively low cost. Therefore, a nominal value of 20% of global annual material supply was assumed to provide a metric to understand the impact of the TW PV production. Sustainable manufacturing capacity SMC_x for each element was then calculated (in GW/year or TW/year) by dividing S_x by C_x , and the element with the lowest SMC (i.e., the limiting material) represented the overall SMC of the corresponding cell technologies. Additionally, the target usage (T_x , in mg/W) for each element was also obtained by dividing 20% global supply by 3 TW assumed annual production to identify

the gaps between current and target usages. Table 1 summarises assumptions and parameters used for this study. Detailed explanations are shown in the texts in supplementary information with parameters listed in Tables S1–S4.

3 | RESULTS AND DISCUSSIONS

Figure 2A illustrates the values for total and 20% of 2020 global annual supply for each critical element identified in this work. The target usages (in mg/W) were also obtained using the method detailed above and are shown in Figure 2B. Take the case of GaAs cells as an example, if such technology could generate annual production of 3 TW and only consume 20% of 2020 global annual supply of gallium and arsenic, the ‘target material consumptions’ for gallium and arsenic under this ideal scenario must be below 0.0218 and 4 mg/W, respectively. The same rules applied to CIGS (copper, indium, gallium and selenium), CdTe (cadmium and tellurium), perovskite (lead and iodine) and silicon cells (silicon). For target usage of metal conductor silver, it is assumed that all the cells contributing to the 3-TW production contain silver metal contacts.

3.1 | Sustainable top cell options

In order to evaluate the material sustainability of top cell options for Si-based tandem devices, critical material usages for III-V, CIGS, CdTe and perovskite candidates were obtained using the methodology detailed in the previous section. The resulting materials consumption and SMC are illustrated in Figure 3, where Figure 3A–C illustrates the

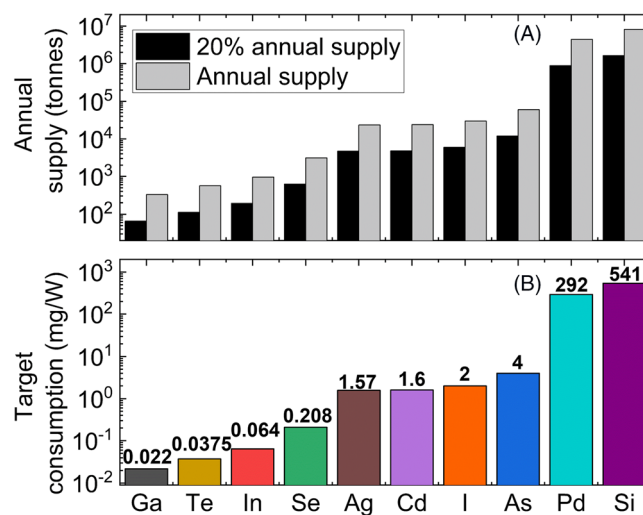


FIGURE 2 (A) Annual primary material supply from USGS 2020 data and with 20% of annual supply for gallium, tellurium, indium, selenium, silver, cadmium, iodine, arsenic, lead and silicon and (B) target consumptions for these materials with assumed annual PV production of 3 TW and only using 20% of their annual supplies.

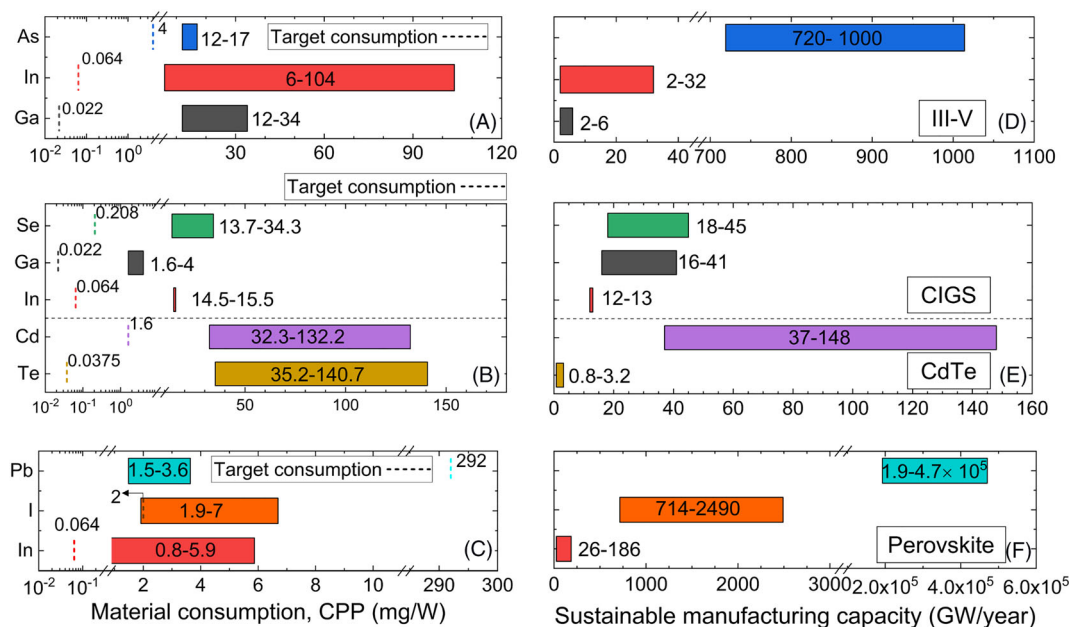


FIGURE 3 Obtained material usages (A–C) and corresponding SMC (D–F) for top cell options of III-V, CIGS, CdTe and perovskites, based on assumptions and parameters described in Table 1.

range of material consumption in mg/W for each material and Figure 3D–F shows the associated range of sustainable manufacture capacity in GW/year when employing these cell technologies. In order to directly compare the target and actual usage for each element, dashed lines in Figure 3A–C indicate the target usage previously shown in Figure 2.

For the III-V group, the target consumption for gallium (Ga), indium (In) and arsenic (As) is approximately 0.022, 0.064 and 4 mg/W, respectively. In practice, GaAs and GaInP/GaInAsP/Si cells consume 12–34 mg/W of Ga and 12–17 mg/W of As, as shown in Figure 3A. These are at least 545 and 3 times the target usages, respectively. The In usage from InP and GaInP/GaInAsP/Si cells ranges from 6 to 104 mg/W, which is 94 to 1625 times larger than the target values. The corresponding SMC for Ga, In and As is 2–6, 2–32, and 720–1000 GW/year, respectively, as shown in Figure 3B. This shows that SMC of III-V group is limited by Ga, with SMC_{Ga} as low as 2–6 GW/year, which means, even if 20% of Ga global annual supply could be employed to fabricate III-V solar cells with the efficiencies as high as 35.9% as listed in Table 1, the maximum production capacity of such solar cells is up to 6 GW/year, which is significantly below the TW/year scale. It is worth noting that this SMC value is relatively conservative due to the following two reasons: First, only a portion of the global Ga supply is refined with high purity and can be used in the manufacturing of III-V group solar cells. For example, the 2020 production of high purity refined Ga was around 214 t,³¹ which was only 65% of the total global Ga supply in the same year (327 t). Second, the material utilisation factor assumed in this work was 80%, which only accounted for the material losses during the epitaxial growth of III-V materials, without considering the losses from electronic grade gallium to trimethyl compounds used as precursors used for III-V epitaxial growth.²¹

CIGS candidates utilise 1.6–4 mg/W of Ga, 13.7–34.3 mg/W of selenium (Se) and 14.5–15.5 mg/W of In as illustrated in Figure 3B. These are over 70, 86 and 223 times of the target values shown Figure 2B for the three materials. As a result, the corresponding SMCs of these three materials are 16–41, 18–45 and 12–13 GW/year, respectively, as shown in Figure 3E. Therefore, the SMC of CIGS solar cells is constrained by Se with an SMC_{Se} of 16–41 GW/year, which is dramatically below the TW/year production goal. Similar limitations arise when comparing the current usage to the target usage of cadmium (Cd) and tellurium (Te) as shown in Figure 3B. CdTe candidates consume 20 to 83 times the target value of Cd and 940–3750 times the target value of Te. The SMC for CdTe technology is hence limited by Te with a SMC_{Te} as low as 0.8–3.2 GW/year as shown in Figure 3E.

The required reductions in material consumption can be achieved either by improving the efficiency or using thinner absorbing layers. For instance, a 19.9% GaAs cell with only 205 nm was fabricated recently.³² However, even with such a thin absorbing layer (20% of the conventional GaAs thickness), the SMC will be only four times higher than the GaAs cells with the conventional thickness and still lower than required for TW deployment. Similarly, neither CIGS nor CdTe cells with their present thickness are feasible as the top cell candidates for TW/year scale Si-based tandem devices.

For perovskite cells, the consumption of lead (Pb) and iodine (I) was considered as the critical elements of the absorbing layers in the forms of $FAPbI_3$ and $CS_{0.05}(FA_{0.77}MA_{0.23}Pb_{0.95}Br_{0.23})_3$. As shown in Figure 3C, the consumption of Pb is 1.5–3.6 mg/W, which is significantly lower than the target value of 292 mg/W, so that the SMC of Pb is 190–470 TW/year as labelled in Figure 3F. The consumption of I is 1.9–7 mg/W, which is 1–3.5 times as that of the

target value of 2 mg/W as listed in Figure 3C, so that the SMC of I is 714–2490 GW/year, as labelled in Figure 3F. If the usage of I can be controlled below 6 mg/W, the corresponding SMC of I will be higher than 1 TW/year. However, perovskite cells require TCO layers to provide lateral conductivity. For the perovskite candidates selected in this work, the ITO thickness ranges from 40 to 285 nm according to the data of 2T and 4T tandem devices listed in Table S2. With the highest efficiency of 25.8% for single junction perovskite cells, indium (In) consumption in this ITO layer equals to 0.8–5.9 mg/W, such that SMC of In for perovskite cells is 26–186 GW/year, as shown in Figure 3E. Therefore, TW/year goal is achievable for perovskite cells only if they are In free and the I usage can be well controlled. Consumption of In in SHJ cells and perovskite/Si tandem cells will be discussed in details in Section 3.4.

In addition to material availability, the toxicity and impact on environment and health of using Pb and solvent must be considered. So far, tin-halide and double-halide perovskites have emerged as two material classes of lead-free alternatives perovskites,³³ Tin-halide perovskite cells have achieved the record efficiency of 14.6%,³⁴ which is significantly lower than that of lead-containing counterpart. More importantly, instability is another critical limitation for lead-free perovskite cells. If lead-free perovskite cells cannot match the stability requirement, lead may still need to be used, but this should be under the condition that lead leakage can be well prevented and managed. More research efforts should be made towards this area, such as using an interlayer in the cell structure,³⁵ physical encapsulations and chemisorption³⁶ and other leakage control measures. In addition, the amount of solvent required for a blade-coated perovskite film is estimated to be 0.5 mL/m², which indicates that 3500 L of solvents are needed for 1 GW of PV generated power assuming that the module is fabricated at high production yield with an efficiency of 15%.³⁷ Among eight types of solvents that are widely used for deposition of organic–inorganic halide perovskites, dimethyl sulfoxide (DMSO) has shown the lowest adverse impact on human health and the environment after a full life cycle analysis (LCA),³⁸ so that the new techniques should be developed to enable high-efficiency perovskite cells with only DMSO or DMSO as the main solvent.

It is also worth mentioning that the use of lead in PV modules processes a greater concern than that used in the perovskite cells, with the lead usage of around 12 g in a standard 60-cell module³⁹ mainly from the lead-based solder, which is equivalent to around 32.4 mg/W with power rating of up to 370 W for such 60-cell modules.⁴⁰ This is significantly higher than that used in the perovskite cells as shown in Figure 3C, so that reducing the lead usage or developing lead-free solder is important. However, lead-free solder currently requires bismuth, which is a type of scarce material,²⁴ whereas lead is also a by-product at zinc and silver mines in addition to lead mines and easy to be recovered.³¹ Therefore, more focus should be given to research not only on lead-free solder alloys made from abundant materials but also on lead leakage prevention and control when no suitable alternative materials can be used.

3.2 | Sustainable silicon bottom silicon cell options

Among three dominant silicon solar cell technologies, PERC, TOPCon and SHJ solar cells involve different structures and fabrication process, and hence, they consume different materials quantities. In addition, adaptations of these three technologies have been used as Si bottom cells in a number of perovskite/Si tandem devices. Therefore, it is worth making comparison among material usages not just for PERC, TOPCon and SHJ cells but also Si bottom cells used in reported perovskite/Si tandem cells. Similar to the material evaluation on top cell candidates, critical material consumptions on Si and silver (Ag) were obtained using the methodology in Section 2 with cell thicknesses, efficiencies, Ag metallisation geometries and cell details listed in Tables 1 and S4. The resulting material consumption and sustainable capacities are illustrated in Figures 4 and 5 for silicon and silver, respectively.

From Figure 4A, it is clear that the Si consumptions for PERC, TOPCon and SHJ are similar, ranging from approximately 2.0 to 2.5 g/W, with the difference primarily attributed to the differences in efficiency as listed in Table 1. On one hand, with the same Si thickness, the advantage of higher efficiency on the reduction of material consumption can be observed from Figure 4. On the other hand, nearly 6% absolute efficiency gain in tandem devices (32.5%) compared with SHJ devices (26.81%) cannot outweigh the disadvantage of the thicker Si wafers that are used for research-scale tandems and which give an upper limit to material consumption as high as 3.16 mg/W. The reason is that the majority of Si bottom cell in the lab-scale perovskite/Si tandem structures is fabricated on Float Zone (FZ) wafers with a thickness up to 300 μ m. This leads to higher Si consumption for tandem devices, which can be more than 66% of Si material than used for single junction SHJ cells (1.9–2.4 g/W, 24.02–26.81% efficient, 150–167 μ m Si). If the bottom cell is fabricated on Czochralski (CZ) wafers with a lower range of the thickness of \sim 150 μ m similar to single junction Si cells, the value could be around 1.64 g/W as labelled in Figure 4A. CZ wafers are hence expected to be employed at large scale for Si-based tandem production, in addition to their compatibility with industrial PV processing in terms of size, thicknesses and cost-effectiveness. This highlights that thickness reductions on silicon cells will continue to be sought after in future PV technology.

As shown in Figure 4B, the SMC_{Si} of PERC, TOPCon and SHJ cells also shares a similar range from 650 to 850 GW/year, whereas the SMC_{Si} for the Si-based tandems shows a wider range of 532–938 GW/year. With the thickness of 150 μ m for silicon bottom and the highest efficiency of 32.5%, the SMC_{Si} for the Si-based tandems can achieve over 1 TW/year. Unfortunately, none of present single junction silicon cell technology can achieve TW/year scale with the current silicon supply in metallic form reported by the US Geological Survey.³¹ What is worse, the assumption that 20% of annual global Si supply could feed into PV industry is also overestimated. In fact, the global Si supply in 2020 shown in Figure 2 consists of both ferrosilicon (an alloy of iron and silicon) and metallurgical-grade (MG) silicon (98% to 99% purity). MG Si is then used for the production of poly-silicon

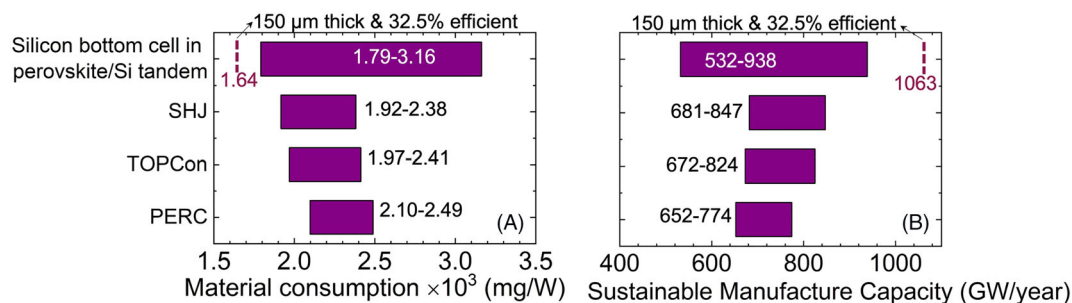


FIGURE 4 Obtained Si material usages (A) and corresponding SMC (B) for single junction PERC, TOPCon and SHJ cells and Si subcells in tandem structures. Based on assumptions and parameters described in Table 1.

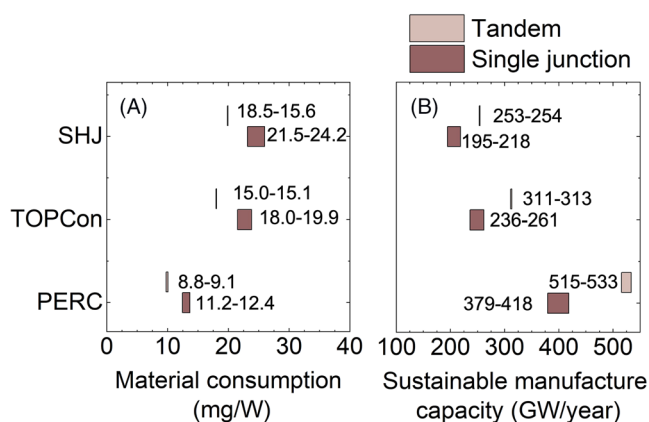


FIGURE 5 Obtained silver material usages (A) and corresponding SMC (B) for bottom cell options of PERC, TOPCon and SHJ cells in a single junction and tandem structures. Based on assumptions and parameters described in Table 1 and assuming tandem devices have the same metal grid geometries as for these three Si cells but with the highest perovskite/Si tandem efficiency of 32.5%.

(poly-Si), for which the demand in 2020 was around 450 kt⁴¹ equating to only 5.5% of total global Si supply (8120 kt) the same year. Out of this, the PV industry uses ~90% of the global poly-Si supply.⁴² The expansion of poly-Si production is expected and inevitable,⁴¹ however, it is worth noting that the large scale and design complexity of poly-silicon production plants result in relatively long lead times of 2.5–6 years from planning to full production, and it takes more than 10 years before any serious levels of production from a new mine can be seen,⁴³ so that the speed of poly-Si expansion may not catch the speed of its demand increase. These figures indicate that research efforts should be put in reducing silicon wafer thickness and increasing material utilisation efficiency³⁰ while the poly-Si production is being expended. Not only is this required to achieve the TW/year target but also to reduce green-house emissions resulting from energy intensive silicon purification.^{44,45}

There are various potential ways to reduce silicon thickness. First, the poly-Si utilisation efficiency can be increased through reducing kerf-loss during the diamond wire sawing and reusing of the kerf-loss.⁴⁶ Second, thinner silicon wafers can be used by engineering cell

manufacturing processes such that breakages are avoided and yield maintained. The low-temperature process used for manufacturing SHJ and perovskite/SHJ tandems can ease the shift to thinner wafers thanks to the better yield achieved in lower temperature processing. The built-in tension after cooling down from a high-temperature firing step results in wafer bowing, which can be too strong for thinner wafers and cause breakage during lamination process.⁴⁷ Besides yield benefits, the improvement in surface passivation in SHJ also benefits the use of thinner wafers, because surface recombination is the dominant recombination mechanism in thin cells.⁴⁸ For instance, a world-record open circuit voltage of 754 mV has been recently achieved by a 56.2- μm -thick SHJ cell (23.27% efficient) with excellent surface passivation via hydrogenated nanocrystalline silicon (nc-Si:H) thin layers.⁴⁹ Studies have shown that with improved light trapping using photonic crystals, over 30% efficiency is achievable on ultra-thin 3- to 20- μm -thick Si solar cells.⁵⁰ Besides, silicon thin film technology provides another pathway to reduce the silicon usage. However, the efficiency of this technology was relatively low, for example, the stabilised efficiency of amorphous silicon modules was only just 7%.⁵¹ Whereas wafer-based Si technologies have been progress so well with largely reduced manufacturing cost, it is hard for thin film amorphous silicon solar cells to compete with wafer-based Si cells. With respect to emissions from poly-Si production, these can be dramatically reduced through using decarbonised electricity to power poly-Si production and purifications and by a transition from conventional Siemens reactors to lower emission options, such as fluidised bed reactor (FBR). Such FBRs can reduce emission by 47.7% per 1 GW of PV modules produced compared with Siemens⁵² and upgraded metallurgical grade (UMG) silicon. For silicon use in photovoltaics, it is likely that even with efforts to reduce wafer thicknesses and increase efficiencies, it will be inevitable to require substantial increases in the production of silicon to meet future demand of the solar industry.

3.3 | Silver electrodes

In 2021, the PV industry used 15% of the global Ag supply⁵³ due to the increased production now reaching 191 GW/year, and the fact that screen-printed silver contact is currently the dominant metallisation technology in silicon solar cells. For PERC, Ag is required for

metal/Si contact formation on the front busbars, electrical conduction in fingers/busbars and in soldering pads for interconnection. On the rear side of PERC, aluminium is used as the fingers and busbars to form bi-facial solar cells, and only a small amount of silver is needed for the solder pads. By contrast, Ag is needed as the busbars and fingers on both sides of the TOPCon and SHJ solar cells, resulting in substantially higher silver consumption than for PERC. Here, Ag consumptions are calculated on single junction PERC (22.99–24.5%^{27,29}), TOPCon (23.71–26.1%^{28,29}), SHJ (24.02–26.81%^{28,29}) and for tandem devices made with same metal grid geometries as for these three Si cells but with the highest perovskite/Si tandem efficiency of 32.5%. All resulting consumption and SMC are plotted in Figure 5. It is worth noting that for the tandem using PERC as the bottom cell, Ag metal contact is only used on the front side of the tandem, while aluminium contact is on the rear side. Detailed silver metal grid dimensions are provided in Table S4.

Figure 5A shows Ag consumptions SHJ, TOPCon and PERC single junction cells to be 21.5–24.2, 18–19.9 and 11.2–12.4 mg/W, respectively. SHJ and TOPCon consume ~2 times and ~1.6 times more Ag than that of PERC. As a result, the corresponding SMC of Ag is 379–418 GW/year for PERC and less than ~220 and 260 GW/year for SHJ and TOPCon, respectively, as shown in Figure 5B. Even if the tandem cell efficiency is 32.5%, the SMC of Ag can only be improved by 1.2–1.4 times, which are equivalent to 515–533, 253–254 and 311–313 GW/year for tandems using Ag grid designs in PERC, SHJ and TOPCon, respectively. These manufacturing capacities are dramatically lower than the TW/year goal, and current usage is considerably higher than the target usage of 1.6 mg/W (Figure 2) for 3 TW_{p.a.} on the basis of using 20% of global Ag supply. Therefore, significant Ag usage reduction is urgently required in order to prevent silver shortage.

Various approaches can reduce silver consumption. First, 2T tandem provides a pathway to reduce silver usage thanks to its low J_{mp}/V_{mp} ratio compared with that of single junction cell based on Equation (1)²⁴:

$$P_{loss_{finger\ Rs}} = \frac{J_{mp}}{V_{mp}} \cdot \frac{\rho_m \cdot \rho_f \cdot W_{cell}^4}{12 \cdot N_{BB}^2 \cdot M_{Ag}} \cdot \eta, \quad (1)$$

which was rearranged to demonstrate a direct impact of the J_{mp}/V_{mp} ratio and silver usage on relative power loss due to cell's finger resistance. Here, J_{mp} and V_{mp} are the current density and voltage of the cell at the maximum power point, respectively, ρ_m is the line resistivity of fingers, ρ_f is the mass density of fingers, N_{BB} represents the number of busbars, W_{cell} is the cell width, M_{Ag} is silver mass consumption in “mg” on fingers, and η represents cell efficiency.

TABLE 2 Reported efficiency (η), current density (J_{mp}) and voltage (V_{mp}) at the maximum power point and the (J_{mp}/V_{mp}) ratio for single junction PERC, TOPCon, SHJ and 2T perovskite/Si tandem devices.

Cell type	η (%)	J_{mp} (A/cm ²)	V_{mp} (V)	J_{mp}/V_{mp} (A/cm ² /V)	Ref
PERC	23.83	0.0398	0.5994	0.0664	54
TOPCon	24.58	0.0384	0.640	0.0600	55,56
SHJ	25.11	0.0377	0.6670	0.0565	57
2T tandem	29.5	0.0178	1.6237	0.0110	58,59

As listed in Table 2, J_{mp}/V_{mp} ratio for a 2T tandem device is roughly 0.011, which is equivalent to approximately one fifth to one sixth as that of single junction silicon cells. Assuming the same parameters of ρ_m , ρ_f , W_{cell} and N_{BB} for the cells in Table 2, 2T tandem devices can allow substantially less M_{Ag} mass to be used, when maintaining the same relative power loss due to finger resistance.

The second approach to reduce the silver usage is to narrow finger width and reduce finger laydown. So far, finger width as narrow as 20 μ m has been achieved by Pattern Transfer Printing (PTP™) technique,^{60–62} which reduces the silver usage in fingers by ~50%. Very low silver laydown has been realised using Rotary Screen Printing⁶³ on SHJ solar cell, such that silver consumption can be reduced to 6–9 mg/W for busbar-less devices.

However, in order to bring the silver usage towards the 1.6 mg/W target, innovative metal grid designs as well as silver-lean or silver-free alternative pastes must be developed for screen printing to continue as the primary metallisation technology. For instance, a seed layer of a silver paste can be screen printed on Si to form metal-silicon interface areas and then capped by a non-silver conductor, or intermittent silver finger can be screen printed to form the metal/silicon interface and then connected by non-silver conductors, which provides lateral conduction to the busbars. Initial developments have shown reductions in the Ag usage to 8 mg/W on PERC cells using innovative finger pattern design.⁶⁴ Options for alternative pastes are potential aluminium paste for p-type poly-Si on oxide (POLO), which can also be adapted to TOPCon cells,⁶⁵ silver-coated copper paste^{66,67} and screen-printable copper paste to form floating copper busbars.⁶⁸ Another approach to reduce silver usage is copper plating, which has been deployed successfully for large-scale production, such as solar cells featuring passivated contacts^{69,70} and SHJ architectures.^{71,72}

3.4 | Indium in ITO layers

Indium is largely used in ITO and zinc-doped indium oxide (IZO) layers as a transparent conductor for perovskite and SHJ solar cells, as well as a recombination layer between the subcells in 2T perovskite/Si tandems. As discussed earlier, availability of indium is a limiting factor of the SMC of perovskite cells. This section will take a closer look at the indium usage in SHJ cells and a number of selected 2T and 4T perovskite/Si tandem devices introduced in Tables 1 and S2, in order to generate a clear picture of the difference between current and target material consumption.

The ITO thicknesses, consumption and SMC for different cell technologies are depicted in Figure 6. For single junction SHJ cells,

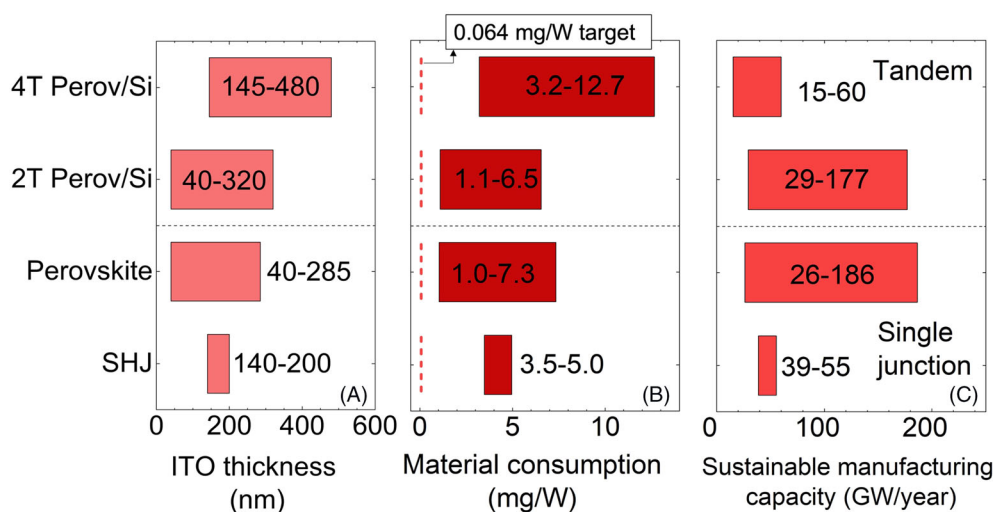


FIGURE 6 (A) ITO thicknesses currently used, (B) calculated in consumption ranges and (C) SMC_{In} for single junction SHJ and perovskite cells, 2T and 4T perovskite/Si tandem cells.

ITO thicknesses are typically 70–100 nm on each side of the solar cells, with the highest efficiency of 26.81%. The In consumption for SHJ cells ranges from 3.5 to 5.0 mg/W as shown in Figure 6B, which is 55–78 times larger than the 0.064 mg/W target value calculated using only 20% of annual global indium supply. The corresponding SMC of In for SHJ is only 39–55 GW/year (Figure 6C), which is lower than the SMC of Ag as shown in Figure 5B. As a result, the SMC of SHJ is constrained by indium, which makes the TW/year scale production goal of SHJ cells even more difficult to hit. As discussed earlier, the consumption of In in 40- to 285-nm-thick ITO layers required for perovskite cells is 1.0–7.3 mg/W, such that SMC of In for perovskite cells is 26–186 GW/year. These are also plotted in Figure 6 in addition to single junction SHJ cells and perovskite/Si tandem cells. The ITO layer thicknesses for 2T perovskite/Si tandem cells range from 40 to 320 nm based on candidates in Table S2. It consists of 40–150 nm on the perovskite top cells, 0–150 nm on the silicon bottom cells, depending on the type of bottom cells (perovskite/TOPCon tandems consume less In than that of perovskite/SHJ tandems), and 0–40 nm as the recombination layer between the two subcells. Details on these thickness calculations are included in Table S3. With efficiencies of 24.5% to 32.5%, the obtained In usages are 1.1–6.5 mg/W, so that the corresponding SMC of In for 2T perovskite/Si tandems is 29–177 GW/year. By contrast, although a recombination layer between the two subcells is not required in a 4T tandem structure, 4T perovskite/Si tandems still consume 145–480 nm ITO, including 80–285 nm on perovskite top cells and 0–230 nm for Si bottom cells based on candidates in Table S2. With efficiencies of 25.2% to 30.1%, the obtained In usages are 3.2–12.7 mg/W, which is 1.9–3 times higher than that of 2T counterpart. Consequently, the corresponding SMC of In for 4T perovskite/Si tandems is as low as 15–60 GW/year. These figures show that with present In usage, it is not feasible to realise TW/year target even if tandem devices achieve the highest efficiency of 32.5%.

To understand the limits of In usage in ITO, the required thicknesses have been calculated and plotted in Figure 7. Consider a tandem cell with an efficiency of 32.5% and targeted In usage of

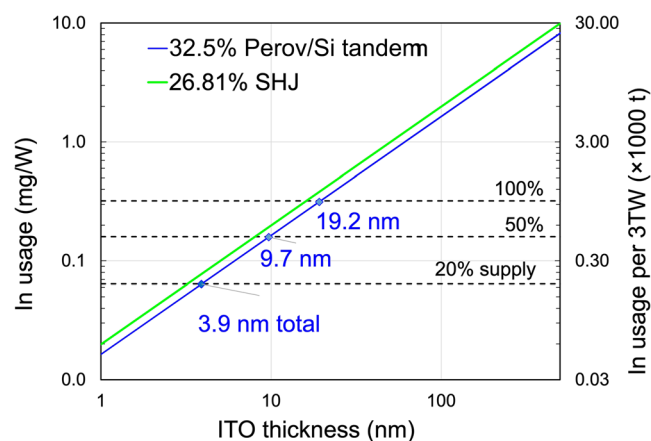


FIGURE 7 Indium usage as a function of ITO thickness for a 26.81% efficient single junction SHJ cell and a 32.5% perovskite/Si tandem cell and corresponding percentage of global indium supply. Numbers in blue indicate that when 32.5% perovskite/Si tandem cells reaching 3-TW annual production and taking up 20%, 50% and 100% of global indium supply, the allowed ITO thickness are 3.9, 9.7 and 19.2 nm per cell, respectively.

0.064 mg/W was calculated based on using only 20% of annual global supply and assumed 3-TW annual production. Given these constraints, only a 3.9-nm-thick ITO layer can be employed for each tandem device, as shown in Figure 7. Deposition of such a thin ITO layer may face uniformity challenge. Additionally, such a thin ITO layer will result in relatively high sheet resistivity ρ_{sheet} and subsequently high power loss due to ITO lateral resistance as shown in Equation (2):

$$P_{loss,ITO_lateral\ Rs} = \frac{\rho_{sheet} \cdot S_f^2 \cdot J_{mp}^2}{12 \cdot V_{mp}}, \quad (2)$$

where S_f represents finger spacing and other terms are defined earlier. Therefore, TCO layers consisting of alternative materials are urgently required. Aluminium-doped zinc oxide (AZO) has been employed on

SHJ cells and demonstrated promising performance as a substitute of ITO,^{58,73,74} including the SHJ bottom cell in the perovskite/Si tandem device with 29.8% world-record efficiency previously. Recently, Longi⁷⁵ also achieved a world-record efficiency of 26.09% for SHJ cells with In-free TCO layer; however, no detailed information regarding the material used were reported.

Similar to the power loss due to finger resistance, the power loss due to ITO lateral resistance is also dependent on J_{mp}/V_{mp} ratio, such that when maintaining the same finger spacing and maintaining the same power loss due to ITO lateral resistance, 2T tandem will allow higher ρ_{sheet} value, in other words thinner ITO or other TCO layer than those employed in single junction devices. This is thanks to the ultra-low J_{mp}/V_{mp} ratio obtained in tandem devices as listed in Table 2. Therefore, 2T tandem configurations are a potential approach to reduce the usage of ITO or other TCO layers.

Another approach to eliminate the use of a TCO layer on the front side of the SHJ solar cells is via a rear-emitter structure design that uses the lateral conduction of Si absorber. Such design has achieved an efficiency over 22% as reported in Li et al.⁷⁶ In addition, a proof-of-concept perovskite/Si tandem without TCO interlayer between the subcells has realised an efficiency of 24.1%.⁷⁷ Based on these examples, it is a reasonable prediction that In-free high efficiency tandems are feasible and have the potential to be realised up to the TW/year production target in the near future.

4 | CONCLUSION

As the era of TW-scale PV manufacturing era rapidly approaches, Si-based tandem solar cells are expected to dominate the next generation of solar PV because of their higher efficiency potential and industrial compatibility for large-scale deployment. One key concern of such a fast and dramatic shift in manufacturing is the increased material consumption. This work investigates the critical material usage for various top cell candidates, Si bottom cells candidates and the requirements associated with silver metal and lateral transport layers based on ITO. From this, the sustainable manufacture capacity, SMC, of various Si-based tandem architectures has been estimated with the assumption that only 20% of the global primary material supply will be required.

Based on our conservative evaluation, SMC of III-V top cell, CIGS and CdTe are below 6 GW/year (limited by Ga), 13 GW/year (limited by In), and 3.2 GW/year (limited by Te), respectively. Therefore, none of these high-efficiency top cell candidates are able to achieve TW-scale production. On the other hand, perovskite solar cells can have SMC values over 1 TW/year, provided their TCO layers are indium-free and usage of iodine can be well controlled. Si consumption in PERC, TOPCon and SHJ are similar, and the corresponding SMC_{Si} is all below 850 GW/year. The majority of the present perovskite/Si tandem cells utilises thick FZ silicon wafers, so that SMC_{Si} in the tandem cells is 532 GW/year. This will be increased to 938 GW/year if CZ wafers are used. With a wafer thickness of 150 μm and efficiency of 32.5%, the SMC of perovskite/Si tandem will achieve 1 TW/year. The SMC of Ag for PERC single junction cells is up to 418 GW/year and below

260 GW/year for TOPCon and SHJ single junction cells. Such SMC can be improved to up to 533, 254 and 313 GW/year for 2T tandems using PERC, SHJ and TOPCon as the bottom cells with present Ag grid designs, respectively. The gain in capacity is largely due to the gain in efficiency and the low J_{mp}/V_{mp} ratio of 2T tandem devices. Indium is the limiting material in the SMC for SHJ single junction cells and perovskite/Si tandem cells, with SMC up to 55 GW/year for SHJ cells and 60 and 177 GW/year for 4T and 2T perovskite/Si tandem configurations, respectively. Therefore, to realise the TW/year target, reductions on silicon wafer thickness and improvement on material utilisation efficiency must be realised. This includes innovative screen-printing metalisation design and Ag-lean pastes, as well as In-free TCO layers such that cell technologies that significantly reduce the demand on Si, Ag and In materials are developed.

It is unclear exactly what percentage of global material annual supply is the most “sustainable” number for PV to consume. A nominal value of 20% of global annual material supply was assumed in this work to provide a metric to understand the impact of the TW PV production. The actual percentage of global material supply for each material and sustainable manufacturing capacity is expected to be dynamic and should be updated accordingly based on new statistics in the future, and the corresponding calculation of SMC can be further optimised, such as with higher efficiencies, thinner wafers, new metalisation designs, new materials and technologies. Other potential candidates consisting of abundant materials, such as CZTSe cells,⁷⁸ CuSbS_2 cells⁷⁹ and other emerging cells may also be feasible for large-scale PV deployment in the future if their efficiencies can be improved significantly. The unexpected today may be a possibility tomorrow.

For PERC technology, it took more than 20 years from achieving world-record efficiency in the laboratory to realising mass production. Although the speed of technology transfer from lab to industry today is faster, it still takes a considerable amount of time to develop new technologies to meet the industry standards for large-scale applications.

The deployment of solar PV in the TW market will primarily be used for electricity generation in rooftop or solar farm settings; however, other markets such as building integrated photovoltaics (BIPV) or space applications may also grow in the future. The design requirements for solar PV in these applications may differ from that of more traditional deployment methods. Assessing other specific cell designs is beyond the scope of this work; however, when considering the materials and resources availability, all PV applications must be viewed in their entirety. The PV community from different sectors should work together to tackle the materials challenges that large-scale PV is facing.

Although some materials are potentially available in the crust and annual supply can be expanded, the environmental impact of such expansion including mining and purification must be evaluated. Additionally, due to the 25- to 30-year lifespan of PV modules, materials used in the PV module have to wait for such a period of time to be recycled if they can be, and there will be material losses during the recycling process. Based on this work, we note that PV is being developed at such a tremendous scale and that more research focus should be shifted from purely improving the efficiency towards improving the sustainable deployment of PV. This must include reducing both

material consumptions and the impacts on environment, society, and human well-being. A compromise of efficiency gain and resources depletion might be a key to open the gate towards TW era photovoltaics deployment.

ACKNOWLEDGEMENTS

This work has been supported by the Australian Centre for Advanced Photovoltaics (ACAP) and the Australian Government through the Australian Renewable Energy Agency (ARENA). Responsibility for the views, information or advice expressed herein is not accepted by the Australian Government. R.S.B was supported by the Royal Academy of Engineering under the Research Fellowship scheme. This work was supported by the UK Engineering and Physical Sciences Research Council grant number EP/V038605/1 and by the John Fell Fund at Oxford University. The authors would like to thank the reviewers for their constructive comments and valuable information to improve this paper. Open access publishing facilitated by University of New South Wales, as part of the Wiley - University of New South Wales agreement via the Council of Australian University Librarians.

DATA AVAILABILITY STATEMENT

The data that supports the findings of this study are available in the supplementary material of this article.

ORCID

Moonyong Kim  <https://orcid.org/0000-0002-3860-5633>

Brett Hallam  <https://orcid.org/0000-0002-4811-5240>

REFERENCES

- <https://unfccc.int/process-and-meetings/the-paris-agreement/the-paris-agreement>
- <https://www.science.org.au/news-and-events/events/climate-change-challenges-health>
- Martin A. Green, how did solar cells get so cheap? *Joule*. 2019;3(3): 631-633. doi:10.1016/j.joule.2019.02.010
- Intergovernmental Panel on Climate Change (IPCC), Climate change 2021: the physical science basis, 2021.
- Global Carbon Budget 2016.
- Green MA. Photovoltaic technology and visions for the future. *Prog Energy*. 2019;1(1):013001. doi:10.1088/2516-1083/ab0fa8
- Verlinden PJ. Future challenges for photovoltaic manufacturing at the terawatt level. *J Renew Sustain Energy*. 2020;12(5):053505. doi:10.1063/5.0020380
- Niewelt T, Steinhäuser B, Richter A, et al. Reassessment of the intrinsic bulk recombination in crystalline silicon. *Sol Energy Mater sol Cell*. 2022;235:111467. doi:10.1016/j.solmat.2021.111467
- <https://www.longi.com/en/news/propelling-the-transformation/>
- Shushnar GJ, Caldwell JH, Reinehl RF, Wilson JH. Balance of system costs for a 5 MW photovoltaic generating system. *IEEE Trans Power Apparatus Syst*. 1985;8(8):2006-2011. doi:10.1109/TPAS.1985.318774
- Shockley W, Queisser HJ. Detailed balance limit of efficiency of *p-n* junction solar cells. *J Appl Phys*. 1961;32(3):510-519. doi:10.1063/1.1736034
- Yu Z, Leilaieoun M, Holman Z. Selecting tandem partners for silicon solar cells. *Nat Energy*. 2016;1(11):16137. doi:10.1038/nenergy.2016.137
- <https://patents.google.com/patent/US9590131B2/en>
- <https://optics.org/news/9/12/19>
- Schygulla P, Muller R, Lackner D, et al. *Prog Photovolt Res Appl*. 2021; 1-11. doi:10.1002/pip.3503
- Green MA, Dunlop ED, Hohl-Ebinger J, Yoshita M, Kopidakis N, Hao X. Solar cell efficiency tables (version 58). *Prog Photovolt Res Appl*. 2021;29(7):657-667. doi:10.1002/pip.3444
- Nakamura M, Yamaguchi K, Kimoto Y, Yasaki Y, Kato T, Sugimoto H. Cd-free Cu(In,Ga)(Se,S)₂ thin-film solar cell with record efficiency of 23.35%. *IEEE J Photovolt*. 2019;9(6):1863-1867. doi:10.1109/JPHOTOV.2019.2937218
- Min H, Lee DY, Kim J, et al. Perovskite solar cells with atomically coherent interlayers on SnO₂ electrodes. *Nature*. 2021;598(7881): 444-450. doi:10.1038/s41586-021-03964-8
- <https://www.pv-magazine.com/2022/12/20/hzb-achieves-world-record-32-5-efficiency-for-perovskite-tandem-solar-cell/>
- <https://www.solliance.eu/2022/four-terminal-perovskite-silicon-pv-tandem-devices-hit-30-efficiency/>
- Zimmermann T. Dynamic material flow analysis of critical metals embodied in thin-film photovoltaic cells: artec-paper Nr. 194. artec Forschungszentrum Nachhaltigkeit. University of Bremen; 2013.
- Gervais E, Shammugam S, Friedrich L, Schlegel T. Raw material needs for the large-scale deployment of photovoltaics—effects of innovation-driven roadmaps on material constraints until 2050. *Renew Sustain Energy Rev*. 2021;137:110589. doi:10.1016/j.rser.2020.110589
- Kamaraki C, Klug MT, Green T, Miranda Perez L, Case C. Perovskite/silicon tandem photovoltaics: technological disruption without business disruption. *Appl Phys Lett*. 2021;119:070501. doi:10.1063/5.0054086
- Zhang Y, Kim M, Wang L, Verlinden P, Hallam B. Design considerations for multi-terawatt scale manufacturing of existing and future photovoltaic technologies: challenges and opportunities related to silver, indium and bismuth consumption. *Energ Environ Sci*. 2021;14(11): 5587-5610. doi:10.1039/D1EE01814K
- <https://www.nrel.gov/pv/cadmium-telluride-solar-cells.html>
- International Technology Roadmap for Photovoltaic (ITRPV) 2021 result, 13 edition, March 2022.
- <https://www.trinasolar.com/en-glb/resources/newsroom/en210-perc-cell-efficiency-achieves-245-trina-solar-breaks-world-record-24th-time#:~:text=Trina%20Solar%20developed%20advanced%20technologies,PERC%20cells%20in%20mass%20production>
- <https://www.pv-magazine.com/2022/10/13/jinkosolar-achieves-26-1-efficiency-for-n-type-topcon-solar-cell/>
- Von Ardenne, Industrial TCOs for SHJ solar cells: approaches for optimizing performance and cost. <https://www.vonardenne.biz/en/company/press-events/industrial-tcos-for-shj-solar-cells/>. (accessed 17 May 2021).
- Hallam B, Kim M, Underwood R, Drury S, Wang L, Dias P. A polysilicon learning curve and the material requirements for broad electrification with photovoltaics by 2050. *Sol RRL*. 2022;6(10):2200458. doi:10.1002/solr.202200458
- U.S. Geological Survey, Mineral Commodity Summary. 2022.
- Chen HL, Cattoni A, de Lépinay R, et al. A 19.9%-efficient ultrathin solar cell based on a 205-nm-thick GaAs absorber and a silver nanostructured back mirror. *Nat Energy*. 2019;4(9):761-767. doi:10.1038/s41560-019-0434-y
- De Angelis F. The prospect of lead-free perovskite photovoltaics. *ACS Energy Lett*. 2021;6(4):1586-1587. doi:10.1021/acsenenergylett.1c00636
- Jiang X, Li H, Zhou Q, et al. One-step synthesis of SnI₂·(DMSO)_x adducts for high-performance tin perovskite solar cells. *J Am Chem Soc*. 2021;143(29):10970-10976. doi:10.1021/jacs.1c03032
- Chen S, Deng Y, Xiao X, Rudd PN, Huang J. Preventing lead leakage with built-in resin layers for sustainable perovskite solar cells. *Nat Sustain*. 2021;4(7):636-643. doi:10.1038/s41893-021-00701-x
- Wu P, Zhang F. Recent advances in lead chemisorption for perovskite solar cells. *Trans Tianjin Univ*. 2022;28(5):341-357. doi:10.1007/s12209-022-00316-z

37. Park N. Green solvent for perovskite solar cell production. *Nat Sustain.* 2021;4(3):192-193. doi:10.1038/s41893-020-00647-6
38. Vidal R, Alberola-Borràs JA, Habisreutinger SN, et al. Assessing health and environmental impacts of solvents for producing perovskite solar cells. *Nat Sustain.* 2021;4(3):277-285. doi:10.1038/s41893-020-00645-8
39. <https://www.pv-magazine.com/2019/10/26/the-weekend-read-a-lead-free-future-for-solar-pv/>
40. <https://www.cleanenergyreviews.info/blog/most-efficient-solar-panels#:~:text=A%20standard%20size%2060%2Dcell,can%20produce%20up%20to%20370W>
41. <https://www.pv-magazine.com/2021/10/26/whats-next-for-polysilicon/>
42. Sandor D, Fulton S, Engel-Cox J, Peck C, Peterson S. System dynamics of polysilicon for solar photovoltaics: a framework for investigating the energy security of renewable energy supply chains. *Sustainability.* 2018;10(1):160. doi:10.3390/su10010160
43. <https://www.ig.com/au/news-and-trade-ideas/commodities-news/lifecycle-of-a-mine--a-step-by-step-guide-to-mining-commodities-180530>
44. Fan M, Yu Z, Ma W, Li L. LCA of crystalline silicon wafers for PV power generation. *Silicon* 2021; 13.
45. Kim M, Storm D, Altermatt P, et al. Identifying methods to reduce emission intensity of centralised PV deployment for net-zero by 2050: Life Cycle Assessment Case Study of a 30 MW PV plant, undereview.
46. <https://www.rosi-solar.com/kerf-recycling/>
47. Fahrner WR. *Amorphous Silicon/Crystalline Silicon Heterojunction Solar Cells*:20. https://books.google.com.au/books?id=UfRHAAAQBAJ&pg=PA20&lpg=PA20&dq=thin+wafer+breaks+at+high+firing+temperature&source=bl&ots=b3O0WW4C2S&sig=ACfU3U33WUWHw5ESIRgPFsrNKIHrbFeikg&hl=en&sa=X&ved=2ahUKewiC4KHS64_5AhUi2DgGHUjgAAwQ6AF6BApEAM#v=onepage&q=thin%20wafer%20breaks%20at%20high%20firing%20temperature&f=false
48. Augusto A, Balaji P, Karas J, Bowden SG. Impact of substrate thickness on the surface passivation in high performance n-type solar cells, 2018 IEEE 7th World Conference on Photovoltaic Energy Conversion (WCPEC) (A Joint Conference of 45th IEEE PVSC, 28th PVSEC & 34th EU PVSEC). 2018;2792-2794. doi:10.1109/PVSC.2018.8548174
49. Sai H, Umishio H, Matsui T. Very thin (56 μm) silicon heterojunction solar cells with an efficiency of 23.3% and an open-circuit voltage of 754 mV. *Sol RRL.* 2021;5(11):2100634. doi:10.1002/solr.202100634
50. Bhattacharya S, John S. Beyond 30% conversion efficiency in silicon solar cells: a numerical demonstration. *Sci Rep.* 2019;9(1):12482. doi:10.1038/s41598-019-48981-w
51. <https://www.pv-magazine.com/2021/04/16/amorphous-silicon-solar-cells-still-niche-market/>
52. <https://www.pv-tech.org/gcl-poly-touts-fbr-silicon-matching-siemens-process-on-purity/#:~:text=The%20reduce%20CO2%20emission%20by,in%2Dhouse%20within%20the%20group>
53. <https://www.silverinstitute.org>
54. Chen R, Tong H, Zhu H, et al. 23.83% efficient mono-PERC incorporating advanced hydrogenation. *Prog Photovolt Res Appl.* 2020;28(12):1239-1247. doi:10.1002/pip.3243
55. Chen D, Chen Y, Wang Z, et al. 24.58% total area efficiency of screen-printed, large area industrial silicon solar cells with the tunnel oxide passivated contacts (i-TOPCon) design. *Sol Energy Mater sol Cells.* 2020;206:110258. doi:10.1016/j.solmat.2019.110258
56. Chen R, Wright M, Chen D, et al. 24.58% efficient commercial n-type silicon solar cells with hydrogenation. *Prog Photovolt.* 2021;29(11):1213-1218. doi:10.1002/pip.3464
57. Ru X, Qu M, Wang J, et al. 25.11% efficiency silicon heterojunction solar cell with low deposition rate intrinsic amorphous silicon buffer layers. *Sol Energy Mater sol Cells.* 2020;215:110643. (SHJ). doi:10.1016/j.solmat.2020.110643
58. <https://www.oxfordpv.com>
59. al-Ashouri A, Köhnen E, Li B, et al. Monolithic perovskite/silicon tandem solar cell with >29% efficiency by enhanced hole extraction. *Science.* 2020;370(6522):1300-1309. doi:10.1126/science.abd4016
60. Adrian A, Rudolph D, Willenbacher N, Lossen J. Finger metallization using pattern transfer printing technology for c-Si solar cell. *IEEE J Photovoltaics.* 2020;10(5):1290-1298. doi:10.1109/JPHOTOV.2020.3007001
61. Mayberry R, Chandrasekaran V. Metallization contributions, requirements, and effects related to pattern transfer printing (PTPTM) on crystalline silicon solar cells, AIP Conf Proc. 2019;2156. doi:10.1063/1.5125873.
62. Lossen J, Matusovsky M, Noy A, Maier C, Bähr M. Pattern transfer printing (PTP™) for c-Si solar cell metallization. *Energy Procedia.* 2015; 67:156-162. doi:10.1016/j.egypro.2015.03.299
63. Lorenz A, Klawitter M, Linse M, et al. Rotary screen printed metallization of heterojunction solar cells: toward high-throughput production with very low silver laydown. *Energ Technol.* 2022;10(8):2200377. doi:10.1002/ente.202200377
64. Hallam, TW workshop slides].
65. Peibst R, Kruse C, Schäfer S, et al. For none, one, or two polarities—how do POLO junctions fit best into industrial Si solar cells? *Prog Photovolt Res Appl.* 2020;28(6):503-516. doi:10.1002/pip.3201
66. Shin J, Kim H, Song KH, Choe J. Synthesis of silver-coated copper particles with thermal oxidation stability for a solar cell conductive paste. *Chem Lett.* 2015;44(9):1223-1225. doi:10.1246/cl.150424
67. Min et al. 38th EUPVSEC 2021.
68. Wood D, Kuzma-Filipek I, Russell R, et al. Passivated busbars from screen-printed low-temperature copper paste. *Energy Procedia.* 2014; 55:724-732. doi:10.1016/j.egypro.2014.08.052
69. Osborne M. Meco's 'cell plating line' enables lower cost high-efficiency solar cells. <https://www.pv-tech.org/mecos-cell-plating-line-enables-lower-cost-high-efficiency-solar-cells/>. (accessed 23 May 2021).
70. Schultz-wittmann O, Turner A, Eggleston B, et al. Proc. 32nd Eur. Photovolt. Sol. Energy Conf., 2016, M, 456-459; D.-H. Neuhaus and A. Münzer, Adv. Optoelectron. 2007, 2007;1-15.
71. TaiyangNews, Heterojunction Solar Technology - 2019 Edition. 2019.
72. Sundrive press release: SunDrive sets 26.07% efficiency record for heterojunction PV cell in mass production – pv magazine International (pv-magazine.com).
73. Wu Z, Duan W, Lambert A, et al. Low-resistivity p-type a-Si: H/AZO hole contact in high-efficiency silicon heterojunction solar cells. *Appl Surf Sci.* 2021;542:148749. doi:10.1016/j.apsusc.2020.148749
74. Nicolay S, Sansonnens L, Sacchetto D, et al. Development of Highly conductive transparent materials for PV applications, CSEM Scientific and Technical Report 2015.
75. <https://www.pv-magazine-australia.com/2022/12/23/longi-claims-worlds-highest-efficiency-for-p-type-indium-free-hjt-solar-cells/>
76. Li S, Pomaska M, Lambert A, et al. Transparent-conductive-oxide-free front contacts for high-efficiency silicon heterojunction solar cells. *Joule.* 2021;5(6):1535-1547. doi:10.1016/j.joule.2021.04.004
77. Shen H, Omelchenko ST, Jacobs DA, et al. In situ recombination junction between p-Si and TiO₂ enables high-efficiency monolithic

perovskite/Si tandem cells. *Sci Adv*, 2018;4:eaau9711. doi:[10.1126/sciadv.aau9711](https://doi.org/10.1126/sciadv.aau9711)

78. https://www.pv-magazine.com/2013/12/11/solar-frontier-breaks-czts-cell-efficiency-record_100013707/

79. doi:[10.1016/j.solmat.2016.02.013](https://doi.org/10.1016/j.solmat.2016.02.013)

SUPPORTING INFORMATION

Additional supporting information can be found online in the Supporting Information section at the end of this article.

How to cite this article: Wang L, Zhang Y, Kim M, et al. Sustainability evaluations on material consumption for terawatt-scale manufacturing of silicon-based tandem solar cells. *Prog Photovolt Res Appl*. 2023;31(12):1442-1454. doi:[10.1002/pip.3687](https://doi.org/10.1002/pip.3687)